Sensors and Materials, Vol. 28, No. 8 (2016) 871–879
MYU Tokyo

S & M 1247

Photo- and Radioluminescence of Sn^{2+} Centers in Alkaline Earth Oxide-Substituted Zinc Phosphate Glass

Hirokazu Masai,* Yuki Ueda, Takayuki Yanagida,[1] Go Okada,[1] and Yomei Tokuda

Institute for Chemical Research, Kyoto University, Gokasho, Uji, Kyoto 611-0011, Japan
[1]Nara Institute of Science and Technology, 8916-5, Takayama-cho, Ikoma, Nara, 630-0192 Japan

(Received January 9, 2016; accepted May 16, 2016)

Keywords: photoluminescence, radioluminescence, glass, Sn^{2+}, alkaline earth oxide

The photoluminescence (PL) and radioluminescence (RL) of Sn^{2+} centers in alkaline earth oxide (*R*O)-substituted ZnO-P_2O_5 glasses, which were prepared under Ar, were examined. We confirm that the network structure of the host glass was changed by the substitution of *R*O for ZnO. Although it seems that the optical absorption is independent of the kind of substituted *R*O, the PL intensities and the PL decay constants suggest that the local coordination state of the Sn^{2+} center is affected by the substitution. From the results of *R*O-substituted SnO-ZnO-P_2O_5 (SZP) glasses, it is expected that an aggregation of Sn^{2+} centers occurs preferentially in a more highly substituted system. The thermally stimulated luminescence of the *R*O-substituted glasses suggests that structural rearrangement during the quenching process induces both aggregation of Sn^{2+} centers and decrease in the number density of traps in the SZP glasses.

1. Introduction

In phosphor applications, the luminescence of materials is observed by irradiation with photons or charged particles.[1] The former with UV–IR excitation is called photoluminescence (PL) and the latter with X-ray or γ-ray excitation is radioluminescence (RL). If higher energy excitation far in excess of the bandgap is applied, the generation of multi-photoelectrons is observed. Such a photoelectron-related process is a characteristic of the RL process, which is different from the conventional PL process. Although the RL process inherently involves (1) the excitation of the host matrix and (2) the energy relaxation process to emission centers, the relaxation process has not yet been clarified. In the RL process, in which visible photons are generated after the energy relaxation process, two types of luminescence have been classified: nonstorage luminescence, i.e., scintillation,[2–5] and storage-type luminescence, such as optically stimulated luminescence (OSL)[6–8] and thermally stimulated luminescence (TSL).[9,10] In the case of storage-type luminescence, energy storage in the trap states governs emission efficiency. In contrast, in scintillation (nonstorage type), it is expected that such defects are a disadvantage for high emission efficiency. Therefore, it is important to examine various luminescence properties using different types of excitation sources.

From the viewpoint of site distribution in solid-state matter, a wider site distribution in amorphous materials is more interesting than that in conventional crystals. Recently, our group has focused on a RE-free amorphous phosphor using ns^2-type cations.[11–19] Because an ns^2 emission

*Corresponding author: e-mail: masai_h@scl.kyoto-u.ac.jp

ISSN 0914-4935

center possesses an electron in the outermost shell in both the ground state (ns^2) and the excited state (ns^1np^1), these types of emission centers are strongly affected by the coordination state. Although we have reported scintillation properties of the ns^2-center-containing oxide glasses,[18,19] their efficiency is insufficient for industrial application. Therefore, control of the local coordination state of the ns^2-type emission center is the key for future applications.

In glass science, it has been suggested that average optical basicity, i.e., the average basicity of oxides in a glass, affects the emission properties of the emission center. For example, divalent metal oxides show a different optical basicity (Λ), which has been defined by Duffy: MgO (0.78), CaO (1.00), SrO (1.10), and BaO (1.15).[20] However, in a previous report,[13] we demonstrated that the PL properties, such as the emission peak energy, of Sn^{2+} centers seem to be independent of the chemical composition of the alkaline earth oxide (*R*O)-substituted ZnO-P_2O_5 glasses. The paper suggested that emission from Sn^{2+} centers is affected by the local basicity of the center, not by the average basicity of the glass. However, this suggestion should be reevaluated, because the preparation was performed in air, in which Sn^{2+} can be oxidized easily into Sn^{4+}.[14] In addition, there was no information about the glass network that may affect the local coordination state of the Sn^{2+} center. Furthermore, examination of PL properties only is insufficient, because both PL and RL measurements may complement each other. On the basis of these considerations, we have precisely examined the correlation between the substituted *R*O content and the PL and RL properties of *R*O-substituted SnO-ZnO-P_2O_5 (SZP) glasses prepared in inert atmosphere. In this study, we also investigated the scintillation and TSL of the SZP glasses as RL measurements for the complete examination of excitation energy flow.

2. Experimental Methods

*R*O (*R* = Mg, Ca, Sr, Ba)-substituted SZP glasses were prepared according to a conventional melt-quenching method that employs a platinum crucible.[14] The chemical composition of the glasses was fixed as 1SnO-*x*RO-(60–*x*)ZnO-40P_2O_5 (*x* = 0–20) (mol%), in which ZnO is substituted by an alkaline earth oxide. Batches consisting of ZnO, $(NH_4)_2HPO_4$, and substitutes such as MgO, $CaCO_3$, $SrCO_3$, and $BaCO_3$ were first mixed and calcined at 1073 K for 3 h. After cooling, SnO was added to the heat-treated solids and the mixture was melted at 1373 K for 30 min in Ar atmosphere. The glass melt was quenched on a stainless steel plate at 473 K and then annealed for 1 h at the glass transition temperature T_g, as measured by differential thermal analysis (DTA).

T_g was measured using a Thermo Plus 8120 (Rigaku) at a heating rate of 10 K/min. Optical absorption spectra were measured using a U-3500 spectrophotometer (Hitachi). PL and PL excitation (PLE) spectra were measured using an F-7000 fluorescence spectrophotometer (Hitachi), whose band pass filter for excitation and emission was 2.5 nm. PL decay curves were measured using Quantaurus-Tau (Hamamatsu Photonics). Internal quantum efficiencies were measured using Quantaurus-QY (Hamamatsu Photonics).The RL spectra obtained by X-ray radiation at room temperature were measured using a monochromator equipped with a charge-coupled device (CCD, Andor DU-420-BU2).[21] The supplied bias voltage and tube current were 40 kV and 5.2 mA, respectively. The irradiation dose was calibrated using an ionization chamber. A pulse X-ray tube (Hamamatsu N5084) and a photomultiplier tube (Hamamatsu R7400) employed as a photodetector were used for the measurement of RL decay curves.[22] The basic concept of the system was the same as that of a pulse X-ray streak camera system,[23] with only the photodetector being changed. OSL spectra were measured after X-ray exposure at 10 Gy using TL-2000 (Nano Gray). The heating rate for the measurement was 1 K/s.

3. Results and Discussion

The obtained *R*O-substituted SZP glasses were colorless and transparent in the visible region. Figure 1(a) shows optical absorption spectra of the 10BaO- and 20BaO-substituted SZP glasses. The optical absorption edge redshifted with increasing substitution. Such a red-shift was observed in all substituent systems. The redshift of the absorption edge due to Sn^{2+} was observed (1) for increases in Sn^{2+} concentration[11,12] or (2) because of aggregation, i.e., spatial disproportionation, of Sn^{2+} centers.[17] It was reported that Sn species in zinc phosphate glasses melted in Ar atmosphere assume the divalent state.[14] Since the present glasses were melted in Ar (purity: 99.999%), all Sn species in the glasses took the divalent state. Thus, it is expected that this redshift mainly originates from an aggregation of Sn^{2+} centers. Figure 1(b) shows optical absorption spectra of the 20*R*O-substituted SZP glasses. In the case of 10*R*O-substituted glasses, no apparent difference was observed. As shown in a previous paper, the optical absorption edge due to Sn^{2+} was barely affected by the type of *R*O substitution.[13] Since the optical absorption edge sensitively reflects the local coordination state of Sn^{2+}, we can conclude that the first neighborhood of Sn^{2+} centers, or that of Sn^{2+} centers interacting with the absorption edge, was not affected by the type of *R*O substitution. This suggests that there is no direct interaction between Sn^{2+} and substituted *R*O species, and that the zinc phosphate network may affect the optical absorption edge.

To examine structural changes in the glass network, ^{31}P magic angle spinning (MAS) nuclear magnetic resonance (NMR) spectra of the glasses were collected. Figure 2(a) shows ^{31}P MAS NMR spectra of the 20*R*O-substituted SZP glasses. The spectra consist of two peaks, which can be assigned to the Q^1 (~12 ppm) and the Q^2 (~28 ppm) phosphorus units.[24,25] As shown in Fig. 2(a), the spectra can be deconvoluted using the Gaussian function. Figure 2(b) shows chemical shifts and half widths at half maximum (HWHMs) of the Q^n peaks as a function of the ionic radii of substituted cations. Because we have not obtained a precise coordination number for the *R*O species, radii values for eight coordination numbers were used in this evaluation.[26] The change in the chemical shift as a result of substitution can be understood from the shielding effect. On the other hand, the structural distribution of phosphorus units decreases with increasing ionic radii, i.e.,

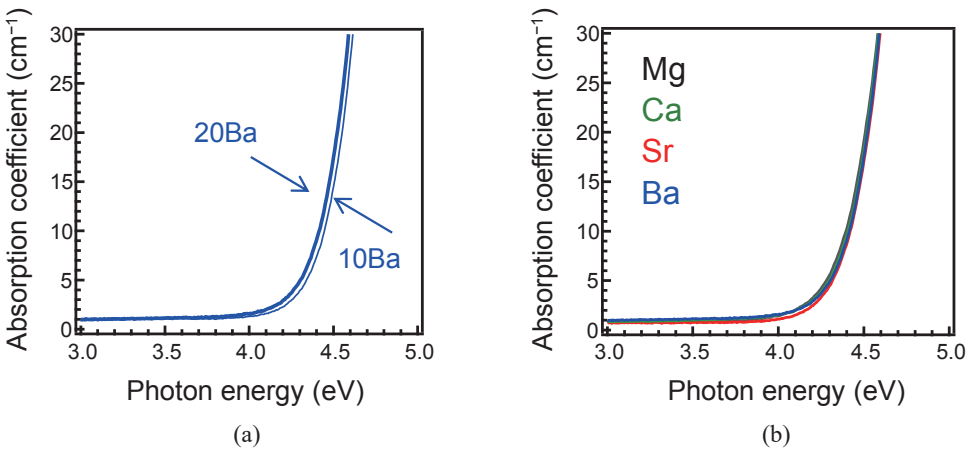

Fig. 1. (Color online) Optical absorption spectra of the *R*O-substituted SZP glasses. (a) Absorption spectra of the 10BaO- and 20BaO-substituted SZP glasses. (b) Absorption spectra of the 20*R*O-substituted SZP glasses.

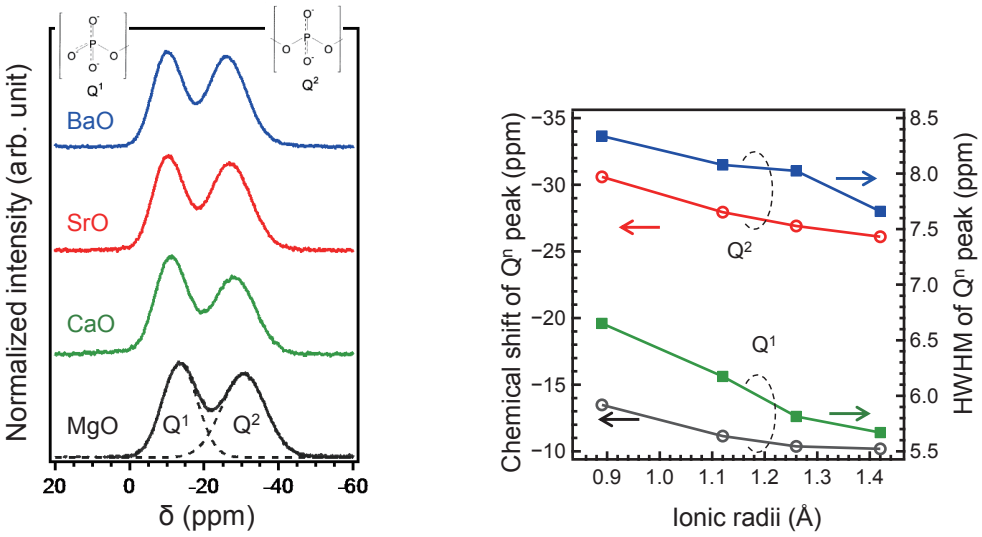

Fig. 2. (Color online) Structural analysis by ^{31}P MAS NMR measurements. (a) ^{31}P MAS NMR spectra of the 20*R*O-substituted SZP glasses. The peak deconvolution of the MgO system is also shown using dashed lines. (b) Chemical shifts and HWHMs of the Q^n peaks as a function of ionic radii of substituted cations.

atomic number. Therefore, it was expected that the structural distribution in Ba-containing glass would be the narrowest among these SZP glasses. On the other hand, for the evaluation of a glass network, the $Q^1/(Q^1+Q^2)$ ratio can be calculated using each peak area. The Q^2 unit constitutes the P–O–P chain network whereas the Q^1 unit possessing a considerably delocalized P=O bond cleaves the chain network. Thus, the $Q^1/(Q^1+Q^2)$ ratio, which also affects the chemical durability,[27,28] is a factor whose value depends on the chemical composition of the glass. We find that the CaO-substituted SZP glass exhibits the highest $Q^1/(Q^1+Q^2)$ ratio. However, at this time, it is difficult to explain the reason for an unchanged absorption edge and the $Q^1/(Q^1+Q^2)$ ratio dependence without information about the random network.

Figure 3(a) shows normalized PL and PLE spectra of the 20*R*O-substituted SZP glasses. We found that no significant peak shift of PLE peaks is observed as a result of the substitution. This indicates that these PLE peaks, i.e., these excitation energy levels, are independent of the element substituted. Although the relative intensity ratio between 5.2 and 4.6 eV varied slightly in a previous study,[13] the variations in these spectra are much smaller than in the previous ones. It is notable that the absorption edges of these glasses also showed little change, which corresponds to a minimal change in the PLE peak energy, which is located in the vicinity of the absorption edge. On the other hand, these PL peak energies were slightly shifted to a lower energy, and the PL bandwidth was broadened by the substitution of heavier cations, as shown in Fig. 3(b). Although these excitation and emission bands are similar, the Mg-substituted glass exhibited the highest intensity, and the PL intensity decreased as a result of the substitution of heavier cations. Comparison of the PL intensities of the 20*R*O-substituted SZP glasses with those of the 10*R*O-substituted glasses showed that the former were lower than the latter. This behavior may be correlated with the aggregation of Sn^{2+} centers.

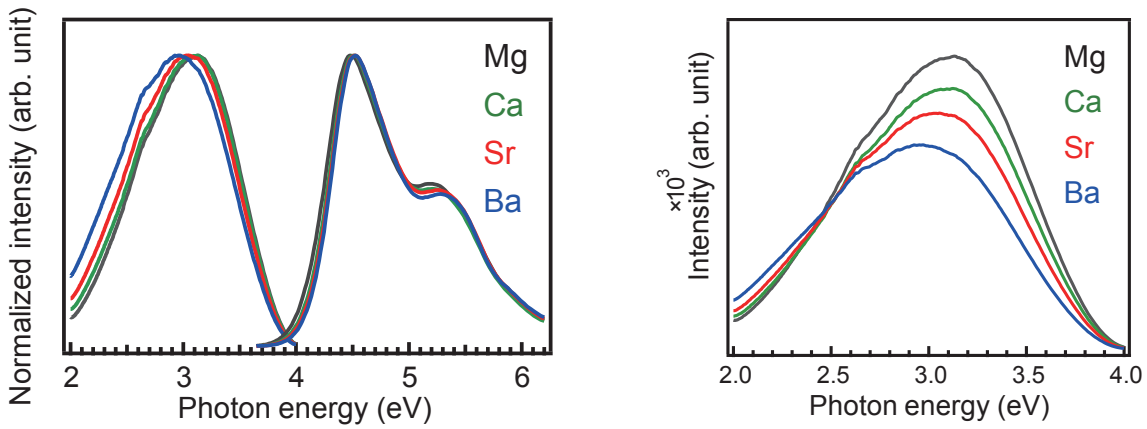

Fig. 3. (Color online) PL and PLE spectra of the *R*O-substituted SZP glasses. (a) PL and PLE spectra of the 20*R*O-substituted SZP glasses. (b) PL spectra of the 20*R*O-substituted SZP glasses without intensity normalization.

Figure 4 shows PL decay curves of the *R*O-substituted SZP glasses: (a) 10*R*O- and (b) 20*R*O- substituted glasses. The excitation and emission of photon energies were 4.4 and 3.0 eV, respectively. The main lifetime $\tau_{1/e}$ of these relaxation processes is on the order of microsecond, indicating that the observed emission may be attributed to a T_1-S_0 transition.[1,15] Although these emission decay curves are similar, the decay constants of these glasses are slightly different. Table 1 shows the decay constants of these glasses. Considering the error bars of an analysis, we find that the 20*R*O-substituted SZP glasses exhibit a lifetime shorter than that of the 10*R*O-substituted glasses, and that Ba-substituted SZP glasses exhibit longer decay constants than the Mg-substituted glasses. Since the oxidation of Sn^{2+} was barely observed under the preparation conditions, it is expected that the coordination state of Sn^{2+} centers in the Ba-substituted system is different from that in the Mg-substituted system, which also affects the differences in PL intensity, as shown in Fig. 3. It has been reported that the Sn^{2+} emission peak shifted toward lower photon energy as time elapsed after UV irradiations.[15,16] Considering the PL spectral shape and the PL decay constant, this assumption about the local coordination state of Sn^{2+} can be explained without contradiction. The shortened lifetime is considered to be correlated to the aggregation of Sn^{2+} species, which is suggested in optical absorption spectra. Although there is no ^{119}Sn Mössbauer spectrum of the Ba-substituted SZP glass, we assume that the origin of these differences is the difference in the local coordination states of Sn^{2+} centers.

Figure 5(a) shows X-ray-induced scintillation spectra of 20BaO-substituted SZP glasses after different irradiation doses as an example. The fitting lines using the Gaussian function are also shown. From the peak fitting, we can obtain peak energy shifts caused by the substitutions. The scintillation peaks were redshifted slightly by the substitution of a heavier cation, which is also observed in PL spectra [Fig. 3(a)]. Figure 5(b) shows the scintillation intensity of the *R*O-substituted SZP glasses as a function of irradiation dose. With increasing irradiation dose, the intensity increased linearly. The inset shows the expanded spectra in the 0.1−0.5 Gy region. It is notable that 10*R*O-substituted glasses exhibited a higher scintillation intensity than the 20*R*O-

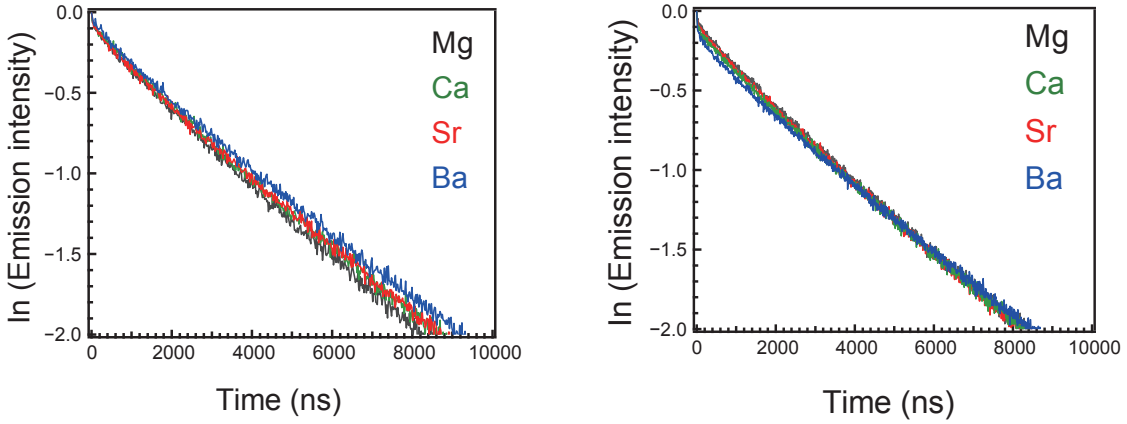

Fig. 4. (Color online) PL decay curves of the *R*O-substituted SZP glasses with 280 nm irradiation: (a) 10*R*O- and (b) 20*R*O-substituted SZP glasses.

Table 1
PL decay constants of the *R*O-substituted SZP glasses. Error bar is ±0.1 μs.

$\tau_{1/e}/\mu_s$	10*R*O	20*R*O
Mg	4.5	4.4
Ca	4.6	4.4
Sr	4.7	4.5
Ba	4.9	4.7

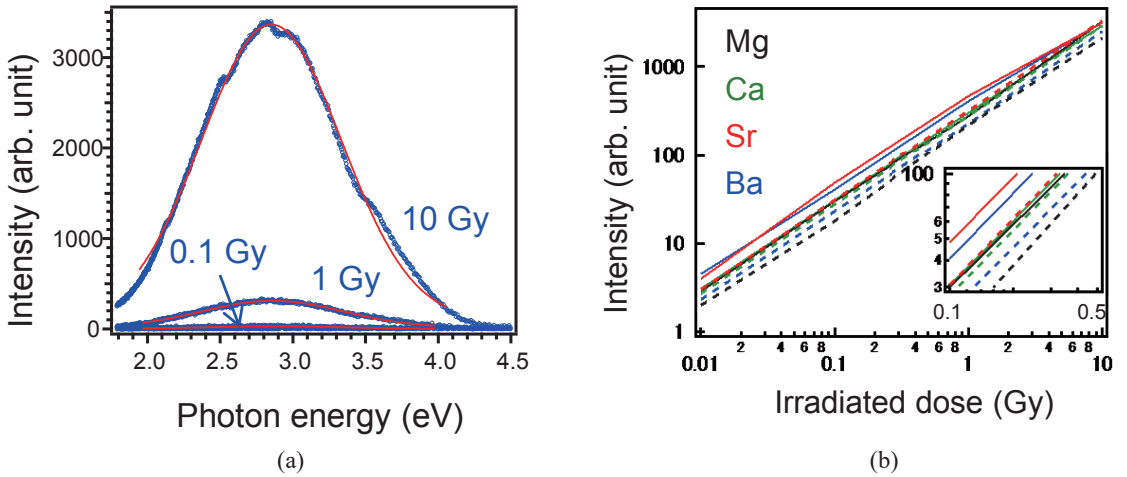

Fig. 5. (Color online) X-ray-induced scintillation spectra of *R*O-substituted SZP glasses after different irradiation doses. (a) Scintillation spectra of the 20BaO-substituted SZP glasses. (b) Scintillation intensity of the *R*O-substituted SZP glasses as a function of irradiation dose. Solid and dashed lines show the data from 10*R*O- and 20*R*O-substituted SZP glasses, respectively. The inset shows the expanded spectra at the 0.1−0.5 Gy region.

substituted glasses. This tendency is consistent with the PL results in which 20*R*O-substituted glasses showed lower intensities and shorter lifetimes because of the aggregation of Sn^{2+} centers.

Figure 6 shows X-ray-induced luminescence decay curves of the 10*R*O-substituted SZP glasses. Since these decay curves consist of at least three components, we evaluated the decay constant of the Sn^{2+} centers as the longest decay component. By curve fitting, the decay constant of Sn^{2+} was estimated to be about 3.4–3.8 μs. Unfortunately, we observed no clear tendency as a function of the substitution.

Figure 7 shows TSL glow curves of *R*O-substituted SZP glasses after 10 Gy irradiation: (a) 10*R*O- and (b) 20*R*O-substituted SZP glasses. From these figures, we found that the shape of TSL glow curves, i.e., trapped states, depended on the amount and identity of the substituted cations.[29] Comparing the two glow curves, we found that the trap depth became larger and that the number density of traps decreased. This observation suggests that the host glass matrix becomes stable with increasing amounts of *R*O. In other words, the structural rearrangement

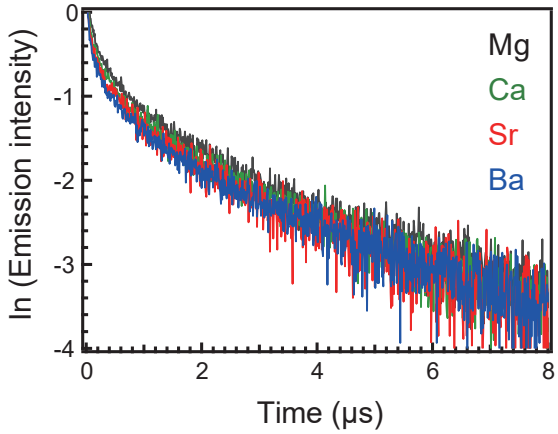

Fig. 6. (Color online) X-ray-induced luminescence decay curves of the 10*R*O-substituted SZP glasses.

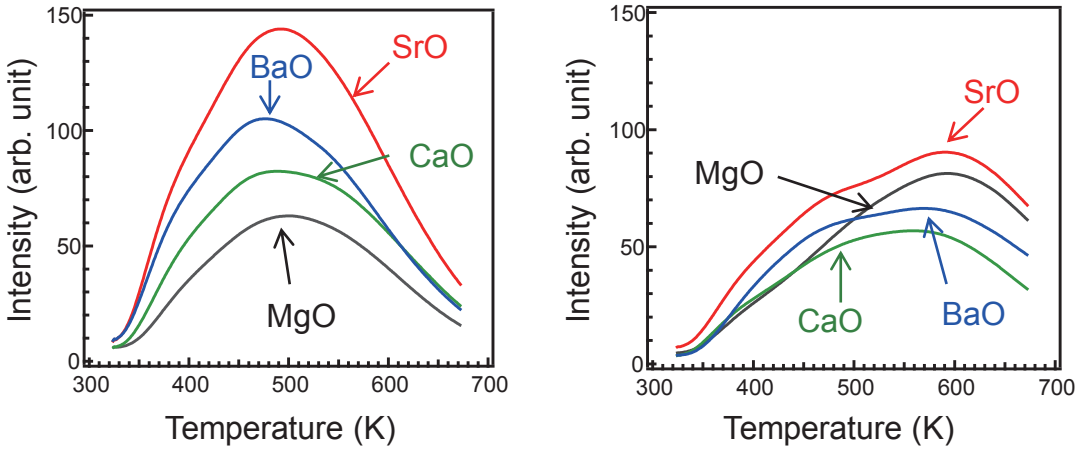

Fig. 7. (Color online) TSL glow curves of *R*O-substituted SZP glasses after 10 Gy irradiation: (a) 10*R*O- and (b) 20*R*O-substituted SZP glasses.

of the glass network occurred easily during the quenching process in the more highly *R*O-substituted system. Considering the network-forming ability of *R*O species, this assumption can be qualitatively understood. In contrast to ZnO, which can act as a network-forming oxide in glass, *R*O species generally have no network-forming ability. Therefore, it is expected that the viscosity of an *R*O-substituted glass melt would be lower than that of a non-substituted one, and that the viscosity would affect the structural rearrangement during the cooling process. The difference in host glass affects not only the optical absorption but also the PL and RL properties of the SZP glasses. Although a strontium-substituted system exhibits the highest intensity among all substituted systems, the reason for this is unclear. Since the Sr cation has been used for a persistent luminescent phosphor,[30,31] some unique effect causing the generation of traps may exist.

4. Conclusions

We have examined the structural and emission properties of *R*O-substituted SZP glasses prepared in Ar. The ^{31}P MAS NMR spectra suggest that the substitution of metal oxides possessing different Λ values leads not only to chemical shift changes but also to the structural distribution of Q^n units. It is expected that the local coordination state of the Sn^{2+} emission center would be affected by the substitution of *R*O, although the effect is barely observed in the optical absorption or PLE spectra. The amount of *R*O substitution affects both the PL and RL properties and strongly correlates with the dispersion of Sn^{2+} centers.

Acknowledgements

This work was partially supported by JSPS KAKENHI Grant-in-Aid for Young Scientists (A) Number 26709048, Collaborative Research Program of I.C.R., Kyoto University (grant #2015-40 and #2016- 83), and the Cooperative Research Project of the Research Institute of Electronics, Shizuoka University. The ^{31}P MAS NMR measurement was performed at Nara Institute of Science and Technology under the Nanotechnology Platform Program of MEXT, Japan.

References

1 Phosphor Handbook, ed. W. M. Yen, S. Shionoya, and H. Yamamoto (CRC Press, Boca Raton, 2007) 2nd ed.
2 G. A. Bray: Anal. Biochem. **1** (1960) 279.
3 M. S. Patterson and R. C. Greene: Anal. Chem. **37** (1965) 854.
4 R. A. Cecil, B. D. Anderson, and R. Madey: Nucl. Instrum. Methods **161** (1979) 439.
5 C. L. Melcher and J. S. Schweitzer: IEEE Trans. Nucl. Sci. **39** (1992) 502.
6 A. S. Murray and A. G. Wintle: Radiat. Meas. **32** (2000) 57.
7 A. G. Wintle and A. S. Murray: Radiat. Meas. **41** (2006) 369.
8 J. Olley, G. Caitcheon, and A. Murray: Quat. Sci. Rev. **17** (1998) 1033.
9 R. Sakai, T. Katsumata, S. Komuro, and T. Morikawa: J. Lumin. **85** (1999) 149.
10 A. G. Wintle: Radiat. Meas. **27** (1997) 769.
11 H. Masai, Y. Takahashi, T. Fujiwara, S. Matsumoto, and T. Yoko: Appl. Phys. Express **3** (2010) 082102.
12 H. Masai, T. Tanimoto, T. Fujiwara, S. Matsumoto, Y. Tokuda, and T. Yoko: Opt. Express **20** (2012) 27319.
13 H. Masai, T. Tanimoto, T. Fujiwara, S. Matsumoto, Y. Tokuda, and T. Yoko: Chem. Lett. **42** (2013) 132.
14 H. Masai, T. Tanimoto, S. Okumura, K. Teramura, S. Matsumoto, T. Yanagida, Y. Tokuda, and T. Yoko: J. Mater. Chem. C **2** (2014) 2137.
15 H. Masai, Y. Yamada, Y. Suzuki, K. Teramura, Y. Kanemitsu, and T. Yoko: Sci. Rep. **3** (2013) 3541.
16 H. Masai, Y. Yamada, T. Tanimoto, Y. Tokuda, Y. Kanemitsu, and T. Yoko: to be published in Sci. Adv. Mater. (2016).

17 H. Masai, A. Koreeda, Y. Fujii, T. Ohkubo, and S. Kohara: Opt. Mater. Express **6** (2016) 1827.
18 H. Masai, T. Yanagida, Y. Fujimoto, M. Koshimizu, and T. Yoko: Appl. Phys. Lett. **101** (2012) 191906.
19 H. Masai, Y. Suzuki, T. Yanagida, and K. Mibu: Bull. Chem. Soc. Jpn. **88** (2015) 1047.
20 J. A. Duffy: Geochim. Cosmochim. Acta **57** (1993) 3961.
21 T. Yanagida, K. Kamada, Y. Fujimoto, H. Yagi, and T. Yanagitani: Opt. Mater. **35** (2013) 2480.
22 T. Yanagida, Y. Fujimoto, T. Ito, K. Uchiyama, and K. Mori: Appl. Phys. Express **7** (2014) 062401.
23 T. Yanagida, Y. Fujimoto, A. Yamaji, N. Kawaguchi, K. Kamada, D. Totsuka, K. Fukuda, K. Yamanoi, R. Nishi, S. Kurosawa, T. Shimizu, and N. Sarukura: Radiat. Meas. **55** (2013) 99.
24 R. J. Kirkpatrick and R. K. Brow: Solid State Nucl. Magn. Reson. **5** (1995) 9.
25 S. M. Hsu, J. J. Wu, S. W. Yung, T. S. Chin, T. Zhang Y. M. Lee, C. M. Chu, and J. Y. Ding: J. Non-Cryst. Solids **358** (2012) 14.
26 D. R. Lide: CRC Handbook of Chemistry and Physics (CRC Press, Boston, 2002) 83rd ed.
27 H. Masai, R. Shirai, K. Yoshida, Y. Takahashi, R. Ihara, T. Fujiwara, Y. Tokuda, and T. Yoko: Chem. Lett. **42** (2013) 1305.
28 H. Masai, R. Shirai, T. Miyazaki, K. Yoshida, T. Fujiwara,Y. Tokuda, and T. Yoko: J. Am. Ceram. Soc. **96** (2013) 3576.
29 H. Nanto, N. Nakagawa, Y. Takei, K. Hirasawa, S. Taniguchi, Y. Miyamoto, H. Masai, T. Kurobori, and T. Yanagida: Proceedings of 2014 IEEE Sensors (2014) p. 416.
30 T. Matsuzawa, Y. Aoki, N. Takeuchi, and Y. Murayama: J. Electrochem. Soc. **143** (1996) 2670.
31 S. H. M. Poort, W. P. Blokpoel, and G. Blasse: Chem. Mater. **7** (1995) 1547.